Free Energies of Urea and of Thermal Unfolding Show That Two Tandem Repeats of Spectrin Are Thermodynamically More Stable Than a Single Repeat†

Ruby I. MacDonald* and Edwin V. Pozharski‡

Department of Biochemistry, Molecular Biology and Cell Biology, 2153 North Campus Drive, Northwestern University, Evanston, Illinois 60208

Received November 1, 2000; Revised Manuscript Received February 5, 2001

ABSTRACT: Free energies of both urea and thermal denaturation have been measured for three pairs of one- and two-repeat fragments, cloned in tandem from the cytoskeletal protein, α-spectrin, from chicken brain to ascertain whether one- and two-repeat fragments are equally stable. One- and two-repeat fragments of each pair were designed with the same N-terminus, whereas the C-terminus of the two-repeat fragment was 106 residues or the length of one repeat downstream from that of the one-repeat fragment. The averaged free energies of urea and thermal denaturation of the paired fragments, $(R16)_{00}$ and $(R16R17)_{00}$, $(R16)_{0+3}$ and $(R16R17)_{0+3}$, and $(R16)_{+8-4}$ and $(R16R17)_{+8-4}$ [subscripts represent the N- and C-terminal positions with "00" referring to the N- and C-termini defining a repeat according to X-ray crystal structures of two repeat fragments [Grum, V. L., Li, D., MacDonald, R. I., and Mondragón, A. (1999) *Cell 98*, 523−535] and "+" and "−" referring to positions upstream and downstream therefrom, respectively], increased from 3.7 ± 0.4 kcal/mol for $(R16)_{00}$, 3.7 ± 0.5 kcal/mol for $(R16)_{0+3}$, 4.4 ± 0.4 kcal/mol for $(R16)_{+8-4}$, 6.2 ± 0.6 kcal/mol for $(R16R17)_{+8-4}$, 8.3 ± 0.4 kcal/mol for $(R16R17)_{00}$ to 9.9 ± 1.0 kcal/mol for $(R16R17)_{0+3}$. Thus, the two-repeat fragment of each pair was significantly more thermodynamically stable than the single repeat by both urea and thermal denaturation. Differences in phasing among single repeats did not have the same effect as the same differences in phasing among two-repeat fragments. Addition of nine residues to the C-terminus of $(R16R17)_{00}$ yielded a free energy of unfolding of 7.9 ± 0.8 kcal/mol, whereas addition of seven residues to the C-terminus of $(R16)_{+8-4}$ yielded a free energy of unfolding of 5.9 ± 0.3 kcal/mol.

The flexibility of the ubiquitous cytoskeletal protein, spectrin, is attributed to elongated domains of 20 and 17 repeating units constituting 90% of α-spectrin and *β*-spectrin, respectively (*1*−*6*). Each repeating unit of 106 amino acids (*7*) is folded into a coiled coil of three, antiparallel α-helices (*8*−*10*) with sequences exhibiting a repeating heptad pattern. Positions in the heptad pattern associated with stability of the coiled coil are "a" and "d", which are occupied by nonpolar residues in interhelical, hydrophobic interactions, and "e" and "g", which are sometimes occupied by charged residues forming salt bridges (*11*). The repeating heptad pattern is absent from linker regions between two repeats, which have been determined by X-ray crystallography to be α-helical in cloned fragments of chicken brain α-spectrin (*12*) and the spectrin-related α-actinin (*13*).

An important advance in promoting the understanding of various aspects of the structure and function of the spectrin-repeating domain at the molecular level has been the cloning thereof of stably folded fragments, the small sizes of which are more amenable to molecular characterization than intact spectrin. As the first to prepare such stably folded, spectrin fragments, Winograd et al. (*14*) demonstrated the importance of "phasing", i.e., selecting from the spectrin cDNA sequence N- and C-terminal positions for the fragment to be cloned so as to facilitate its stable folding. Fragments with N- and C-termini far from those positions displayed higher protease sensitivity and lower α-helical structure by circular dichroism (CD) than more optimally phased fragments (*14*). Since then, extensive application of this approach to the biophysical and biochemical characterization of fragments of the spectrin repeating unit domain has provided significant insights into its structure and function (*15*, *16*).

The properties of spectrin addressed here are the thermodynamic stabilities of cloned fragments of the repeating unit domain which have been studied by urea (*17*, *18*) and by thermal (*19*−*21*) denaturation. Still unanswered questions to emerge from these protein unfolding studies are (1) whether urea and thermal denaturation of these peptides yield the same free energies of unfolding, i.e., indicate the same thermodynamic stability, (2) whether a two-repeat fragment is thermodynamically more stable than a one-repeat fragment, and (3) precisely which N- and C-terminal positions are correlated with maximal stability in terms of free energies of denaturation—what might be termed "microphasing", in contrast with the "macrophasing" of Winograd et al. (*14*). Urea denaturation curves have been interpreted to indicate that two-repeat fragments are "more stable" than a single repeat (*17*), whereas thermal denaturation curves showed that

† This work was supported by grants to R.I.M. from the American Heart Association, Chicago Affiliate, and from the NIH (GM57692).

* Corresponding author: phone (847) 491-2871; fax (847) 467-1380; e-mail rubymacd@northwestern.edu.

‡ Current address: Rosenstiel Basic Medical Science Research Center, Brandeis University, 415 South St., Waltham, MA 02454.

10.1021/bi0025159 CCC: $20.00
Published on Web 03/09/2001

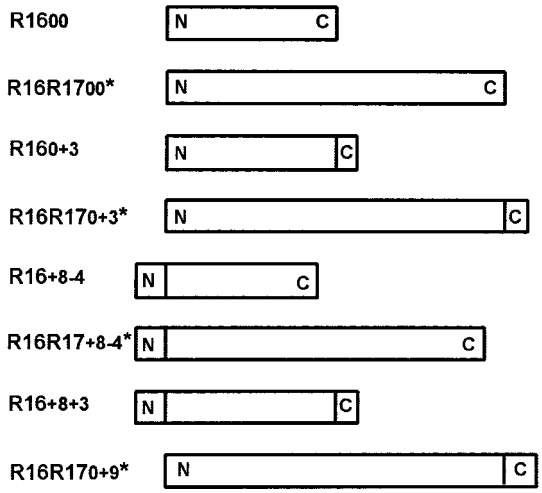

FIGURE 1: Diagram of the phasing of the eight constructs prepared for this study. The rods labeled $(R16)_{00}$ and $(R16R17)_{00}$ represent their linear sequences of 106 and 212 residues, respectively. Additions to and/or deletions from the other constructs are indicated by lengthening and/or shortening of those rods, respectively. The N- and C-termini are labeled. Asterisks indicate constructs, the structures of which were determined by X-ray crystallography (*12*). In that study $(R16R17)_{00}$ was referred to as $2U_{-8+4}$, $(R16R17)_{0+3}$ as $2U_{-8+7}$, $(R16R17)_{+8-4}$ as $2U_0$, and $(R16R17)_{0+9}$ as $2U_{-8+13}$.

a single repeat is as thermally stable as the intact α-spectrin dimer (*19*). In another thermal denaturation study the denaturation temperature of a fragment was not correlated with the number of repeats comprising the fragment, so that single repeats were judged not to be consistently less thermally stable than multiple repeats (*20*). Whether two repeats are more thermodynamically stable than a single repeat deserves investigation as the answer could have implications for cooperativity among repeats which, in turn, may have clinical significance, as indicated in the Discussion.

To resolve the discrepancy concerning the thermal stabilities of one vs two repeating units of spectrin, it appeared necessary to determine the free energies of urea denaturation and of thermal denaturation of such peptides. We report here the free energies of unfolding for three pairs of identically phased, one- and two-repeat fragments—i.e., both fragments in the pair have the same N-terminus, whereas the C-terminus of the two-repeat fragment is 106 residues, the length of one repeat (*7*), downstream of the C-terminus of the single-repeat fragment—for a rigorous comparison of the fragments in each pair, which was phased slightly differently from the other pairs. We have found for each pair that the free energy of unfolding of the two-repeat fragment is significantly greater than that of the single repeat with the same phasing, leaving no doubt that a two-repeat fragment is thermodynamically more stable than a single repeat. Furthermore, the free energy of unfolding of each repeat is the same whether obtained by urea-induced unfolding or by thermal unfolding. These and other results indicate that molecular interactions between repeats, which have been observed in X-ray crystal structures of two-repeat fragments (*12*), may enhance the thermodynamic stability of the repeating unit motif, as well as its potential for cooperative behavior and flexibility.

EXPERIMENTAL PROCEDURES

Design of Peptides. Of the eight spectrin peptides cloned from chicken brain α-spectrin for this study (Figure 1), three pairs of one- and two-repeat fragments were designed with the fragments of each pair being identically phased—i.e., possessing the same N-terminus but the C-termini of which are separated by 106 residues, the length of a single repeating unit (*7*). Each pair was phased slightly differently from the other pairs. This design was intended to test whether such shifts in phasing would affect the relative thermodynamic stabilities of folding of identically phased one- and two-repeat fragments as suggested by others (*19*). For this report, therefore, we have named the fragments according to whether they consist of one repeat (R16) or two repeats (R16R17) and according to their N- and C-termini by the two subscripts following the name of each construct. [R16 and R17 are the 16th and 17th repeats, respectively, of chicken brain α-spectrin (*22*).] The subscript designation "00" refers to positions identified in the X-ray crystal structures of repeats 16 and 17 in tandem (*12*), the first "0" representing the N-terminus, which is the first residue of the repeating heptad pattern of the first α-helix of R16, and the second "0" representing the C-terminus, which is the last residue of R16 or R17 before the first residue of the next repeat in the cDNA sequence. Thus, the N-terminus of $(R16)_{00}$, $(R16R17)_{00}$, $(R16)_{0+3}$, $(R16R17)_{0+3}$, and $(R16R17)_{0+9}$ is residue 1771 in the cDNA sequence. The C-termini of $(R16)_{00}$ and $(R16)_{0+3}$ are residues 1876 and 1879, respectively, and of $(R16R17)_{00}$, $(R16R17)_{0+3}$, and $(R16R17)_{0+9}$ are residues 1982, 1985, and 1991, respectively. $(R16)_{+8-4}$ spans residues 1763−1872. The identically phased two-repeat fragment, $(R16R17)_{+8-4}$, includes residues 1763−1978. An unpaired repeat with the same N-terminus, $(R16)_{+8+3}$, was extended at its C-terminus to residue 1879. The two unit constructs, $(R16R17)_{+8-4}$, $(R16R17)_{00}$, $(R16R17)_{0+3}$, and $(R16R17)_{0+9}$, were previously referred to as $2U_0$, $2U_{-8+4}$, $2U_{-8+7}$, and $2U_{-8+13}$, respectively, in the publication describing their crystal structures (*12*).

Cloning, Expression, and Purification of Spectrin Peptides. Cloning, expression, and purification of spectrin peptides were performed as previously (*18*, *23*). Chicken brain α-spectrin cDNA (*22*) used in PCR amplification of each construct was a kind gift from Dr. Matti Saraste. Expression in *Escherichia coli* BL21DE3 of pET3d, ligated to a spectrin cDNA construct, was induced with IPTG. Peptides released from the pelleted and resuspended cells by sonication were purified by ion-exchange chromatography on DEAE- and Q-Sepharose columns and by gel filtration on a Sephacryl S-100 column. All peptides were >99% pure by SDS−PAGE. cDNA sequencing of each construct revealed no mutations in the single unit constructs or $(R16R17)_{+8-4}$ but mutations G1827S in $(R16R17)_{00}$, K1833M in $(R16R17)_{0+3}$, and K1861E in $(R16R17)_{0+9}$. These mutations were not in positions critical to conformational stability. The N-terminus represented by "0" was valine, instead of leucine, in order to use the restriction enzyme *Nco*I. Percent differences between the mass expected for each peptide from that measured by mass spectrometry were 0.18, 1.1, 1.1, 0.45, 0.2, 0.46, 0.9, and 0.0 for $(R16)_{+8-4}$, $(R16)_{00}$, $(R16)_{0+3}$, $(R16R17)_{+8-4}$, $(R16R17)_{00}$, $(R16R17)_{0+3}$, $(R16R17)_{0+9}$, and $(R16)_{+8+3}$, respectively. To determine whether the peptides were monomers in solution, they were sedimented to equilibrium in a Beckman XL-A analytical ultracentrifuge at 20 °C in 0.1 M NaCl + 10 mM sodium phosphate, pH 8, and the apparent molecular mass, $M_{w,app}$, of each was

obtained by fitting the data with the Microcal Origin program to the equation for a single, ideally behaving species, $A_x = A_0 \exp[HM_{w,app}(x^2 - x_0^2)] + E$, where A_x is the A_{280nm} at radius x, A_0 is the A_{280nm} at the reference radius x_0, H is a constant, and E is the baseline offset. Light scattering of the peptides remains the same in the presence or absence of 0.1 M NaCl, as observed by others (*20*) of similar peptides, indicating that our peptides are also monomers in 10 mM sodium phosphate, pH 8.

Circular Dichroism Measurements. Measurements of circular dichroism at 222 nm of urea-treated peptides at 5 μM in 10 mM sodium phosphate, pH 8, were made in a Jasco J715 spectropolarimeter at room temperature with a cell of 1 mm path length, as previously (*18*). The instrument was calibrated with *d*-10-camphorsulfonic acid. Thermal denaturation of peptides at 1−3 μM in 10 mM sodium phosphate, pH 8, and stirred with a magnetic bar in a cell of 1 cm path length was controlled by a Peltier device supported by a circulating water bath and monitored with a temperature probe in the sample. CD_{222nm} values, corrected for the buffer, were converted into fraction of unfolded values to facilitate comparison of denaturation curves.

Fluorescence Measurements. Tryptophan fluorescence of the same urea-denatured samples monitored by CD was excited at 295 nm and the emission scanned from 300 to 400 nm in an AlphaScan spectrofluorimeter (Photon Technologies International, Inc.) at room temperature, as previously (*18*). Fluorescence emission intensities at 330 or 354 nm, corrected for light scattering, Raman, and buffer contributions, were converted into fraction of unfolded values to facilitate comparison of various denaturation curves.

Analysis of Urea Denaturation Data. As previously (*18*), the method of Jackson et al. (*24*) was followed in which the CD or fluorescence signal, y, plotted as a function of the urea concentration, U, is given by eq 1 for a two-state, reversible process:

$$y = \{(\alpha_N + \beta_N U) + (\alpha_D + \beta_D U) \exp[(mU - mU_{50\%})/RT]\}/\{1 + \exp[(mU - mU_{50\%})/RT]\} \quad (1)$$

where α is the y intercept of the native (N) or denatured (D) state, β is the slope of the native (N) or denatured (D) state, $U_{50\%}$ is the urea concentration at the midpoint of urea denaturation, m is the slope of the transition, native ↔ denatured, R is the gas constant, 1.987 cal·mol^{-1}·K^{-1}, and T is the temperature in K. The parameters $U_{50\%}$ and m were obtained by nonlinear regression fitting of the data to eq 1 with SigmaPlot 4.0 in Windows. The free energy of denaturation, ΔG_{UN}, in the absence of urea is the product of $U_{50\%}$ and m.

Analysis of Temperature Denaturation Data. The free energy of protein denaturation, ΔG_{UN}, is the difference between the free energy of the native state, G_A, and the free energy of the denatured state, G_B (*25*). The relative concentrations of the two states, A and B, expressed in terms of the relationship between the equilibrium constant, K, and the free energy of the transition, ΔG_{UN}, are $A = \{1 + \exp(-\Delta G_{UN}/RT)\}^{-1}$ and $B = \{1 + \exp(\Delta G_{UN}/RT)\}^{-1}$. If it is assumed that states A and B have a linear dependence on temperature over the range in which the protein denatures—i.e., $y_A = \alpha_N + \beta_N T$ and $y_B = \alpha_D + \beta_D T$—the observed signal, y, at any temperature, T, in K is given by

$$y = (\alpha_N + \beta_N T)/\{1 + \exp(-\Delta G_{UN}/RT)\} + (\alpha_D + \beta_D T)/\{1 + \exp(\Delta G_{UN}/RT)\} \quad (2)$$

Following from $\Delta G = \Delta H - T\Delta S$, and using $\delta S = \Delta S/R$ and $\delta H = \Delta H/R$, eq 2 is rewritten as

$$y = (\alpha_N + \beta_N T)/\{1 + \exp(\delta S - \delta H/T)\} + (\alpha_D + \beta_D T)/\{1 + \exp(\delta H/T - \delta S)\} \quad (3)$$

When $\Delta G_{UN} = 0$ and $T = T_m$, the melting temperature at the midpoint of thermal denaturation, $\delta S = \delta H/T_m$. Similarly, δH is given from the van't Hoff equation as $\delta H = 4T_m^2/\Delta T$, where ΔT is the width of the transition. To facilitate nonlinear regression fitting of the data, eq 3 can be rewritten in terms of T:

$$y = (\alpha_N + \beta_N T)/\{1 + \exp(4T_m(T - T_m)/T\Delta T)\} + (\alpha_D + \beta_D T)/\{1 + \exp(4T_m(T_m - T)/T\Delta T)\} \quad (4)$$

where y can be the CD signal at 222 nm. After T_m was obtained by nonlinear regression fitting of the data to eq 4 with SigmaPlot 4.0 in Windows, ΔG_{UN} was calculated from the equation:

$$\Delta G_{UN} = 4RT_m(T_m - T)/\Delta T \quad (5)$$

Table 1: Mean Residue Ellipticities of Cloned Spectrin Fragments at 222 nm

peptide	θ^a	%^{b} of max θ
$(R16)_{+8-4}$	−21 600 ± 1200	60
$(R16R17)_{+8-4}$	−24 000 ± 0	67
$(R16)_{00}$	−24 900 ± 0	69
$(R16R17)_{00}$	−27 100 ± 2100	75
$(R16)_{0+3}$	−25 900 ± 0	72
$(R16R17)_{0+3}$	−25 100 ± 100	70
$(R16)_{+8+3}$	−26 600 ± 800	74
$(R16R17)_{0+9}$	−25 700 ± 1000	71

[a] Average mean residue ellipticity ± standard error in deg·cm^2·dmol^{-1} calculated from urea and temperature-induced unfolding data. [b] Average mean residue ellipticity divided by −36 000 deg·cm^2·dmol^{-1} (*26*) and multiplied by 100.

RESULTS

Properties of Spectrin Peptides. All eight spectrin peptides depicted in Figure 1 displayed CD spectra with a typically α-helical signature of a maximum at about 194 nm and two minima at about 208 and 222 nm, respectively (Figure 2A). The average mean residue ellipticities at 222 nm ± standard errors are listed in Table 1 with the percent α-helicity calculated therefrom, based on −36 000 deg·cm^2·dmol^{-1} as the maximum value given by an α-helical peptide (*26*). The percent α-helicity ranged from 60% for $(R16)_{+8-4}$ to 75% for $(R16R17)_{00}$, which is typical for stably folded spectrin repeats (e.g., refs *18*, *21*, and *23*). There was no consistent correlation between the mean residue ellipticity at 222 nm of a peptide in Table 1 and its free energy of urea or thermal unfolding in Table 2. All eight peptides also exhibited spectra of solvent-shielded tryptophans in Figure 2B with emission maxima at about 330 nm with one exception. The spectrum of $(R16R17)_{0+9}$ appears to consist of two peaks, one at 330 nm and a second one at about 350 nm, the latter due to a

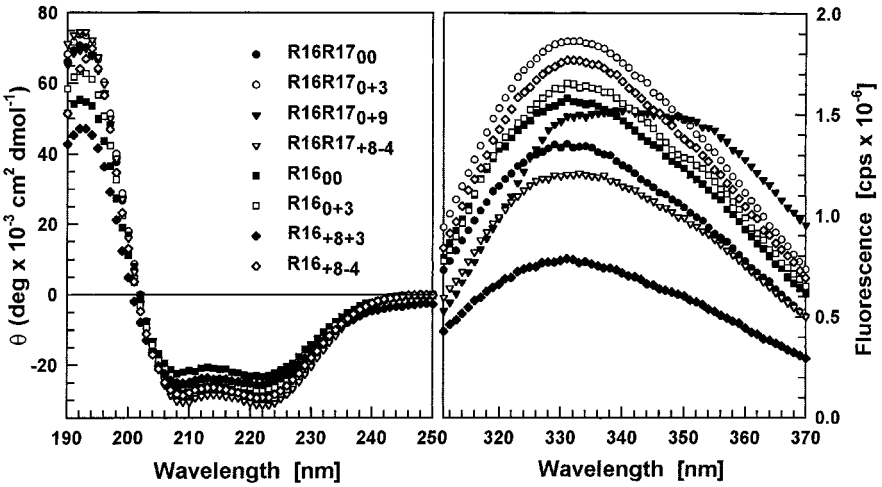

FIGURE 2: (A, left) CD spectra of all peptides at 5 μM in 10 mM sodium phosphate, pH 8, at room temperature. (B, right) Tryptophan fluorescence emission spectra on excitation at 295 nm of all peptides at 5 μM in 10 mM sodium phosphate, pH 8, at room temperature. The legend in panel A also applies to panel B.

Table 2: Free Energies of Urea and Thermal Denaturation of Spectrin Peptides

peptide	ΔG_{UN}^{CD} from urea[a]	ΔG_{UN}^{FL} from urea[b]	ΔG_{UN} from heating[c]	av ΔG_{UN}[d]
$(R16)_{+8-4}$	4.2 ± 0.8	4.7 ± 0.6	4.2 ± 0.0	4.4 ± 0.4
$(R16R17)_{+8-4}$	6.4 ± 0.3	6.7 ± 0.4	5.6 ± 0.1	6.2 ± 0.6
$(R16)_{00}$	3.5 ± 0.3	3.4 ± 0.4	4.1 ± 0.0	3.7 ± 0.4
$(R16R17)_{00}$	8.5 ± 0.7	8.4 ± 0.7	8.1 ± 0.1	8.3 ± 0.4
$(R16)_{0+3}$	3.4 ± 0.3	3.4 ± 0.1	4.4 ± 0.0	3.7 ± 0.5
$(R16R17)_{0+3}$	9.5 ± 1.7	9.4 ± 1.2	10.8 ± 0.2	9.9 ± 1.0
$(R16)_{+8+3}$	6.0 ± 0.8	5.9 ± 0.6	5.9 ± 0.0	5.9 ± 0.3
$(R16R17)_{0+9}$	7.2 ± 0.7	7.8 ± 0.5	8.6 ± 0.1	7.9 ± 0.8

[a] Free energy of denaturation by urea ± standard error in kcal/mol at 25 °C monitored by CD_{222nm}. [b] Free energy of denaturation by urea ± standard error in kcal/mol at 25 °C monitored by tryptophan fluorescence. [c] Free energy of thermal denaturation ± standard error in kcal/mol at 25 °C monitored by CD_{222nm}. [d] Free energy of denaturation ± standard error in kcal/mol at 25 °C averaged from free energies of denaturation in the columns to the left.

tryptophan on the C-terminal, helical extension which is surrounded by solvent (*12*) so that its emission maximum is red shifted. The shielded tryptophans in the different peptides are quenched to different extents. Both the CD and tryptophan spectra indicate that all of the peptides are well folded.

Analytical ultracentrifugation of the peptides to sedimentation equilibrium indicated that each peptide is a monomer in solution. The following apparent molecular masses, $M_{w,app}$, of the spectrin peptides in daltons, with χ^2 values of the corresponding fits in parentheses, were 11 892 (1.8e-4) for $(R16)_{00}$, 11 592 (5.8e-5) for $(R16)_{0+3}$, 21 072 (2.0e-4) for $(R16R17)_{+8-4}$, 21 882 (6.1e-5) for $(R16R17)_{00}$, 22 702 (5.3e-5) for $(R16R17)_{0+3}$, 23 687 (5.6e-5) for $(R16R17)_{0+9}$, and 12 930 (1.8e-4) for $(R16)_{+8+3}$. These values are within 15% of those expected. $(R16)_{+8-4}$ has been shown to be a monomer in solution by light scattering (*23*) and by analytical ultracentrifugation (*10*).

Urea Denaturation of Pairs of Identically Phased, One- and Two-Repeat Spectrin Fragments Monitored by Circular Dichroism at 222 nm and by Tryptophan Fluorescence. Each panel of Figure 3 shows the urea denaturation curves, monitored by CD_{222nm} and by tryptophan fluorescence, of a pair of identically phased one- and two-repeat chicken brain

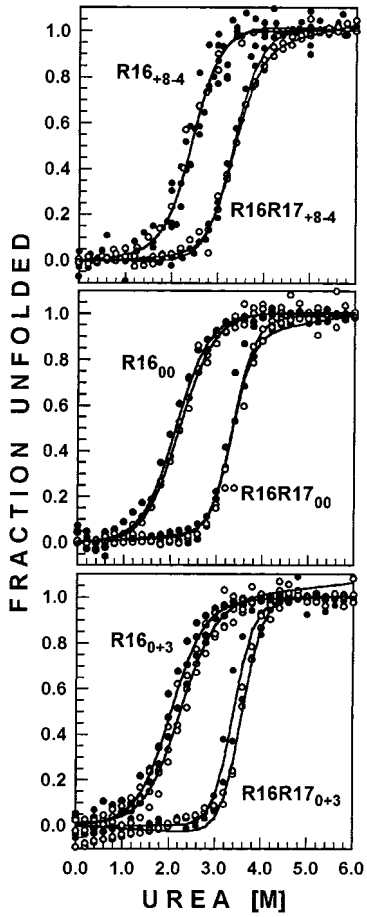

FIGURE 3: Fraction unfolded values of $(R16)_{+8-4}$, $(R16R17)_{+8-4}$, $(R16)_{00}$, $(R16R17)_{00}$, $(R16)_{0+3}$, and $(R16R17)_{0+3}$ plotted against urea concentration with a curve (solid line) describing the best fit of the data to eq 1 (Experimental Procedures). Open circles represent values based on CD_{222nm}, and closed circles represent values based on tryptophan fluorescence.

α-spectrin peptides. The CD_{222nm} and tryptophan fluorescence of each peptide at 5 μM in 10 mM sodium phosphate, pH 8, were measured at room temperature following overnight equilibration with urea at concentrations from 0 to 6.0 M. These data were converted into fraction unfolded values, which are plotted versus urea concentrations in Figure 3: CD_{222nm} as open circles and tryptophan fluorescence as filled

Table 3: Thermodynamic Parameters Correlated with Free Energy of Unfolding, ΔG_{UN}

	urea denaturation		heat denaturation	
peptide	m[a]	$U_{50\%}$[b]	T_m[c]	ΔT[d]
$(R16)_{+8-4}$	1960	2.4	51.4	14.9
$(R16R17)_{+8-4}$	2038	3.3	52.0	12.5
$(R16)_{00}$	1624	2.2	49.0	15.0
$(R16R17)_{00}$	2506	3.5	52.0	8.6
$(R16)_{0+3}$	1589	2.1	49.3	14.1
$(R16R17)_{0+3}$	3069	3.3	53.4	6.8
$(R16)_{+8+3}$	1973	3.1	54.0	12.7
$(R16R17)_{0+9}$	2258	3.4	51.8	8.0

[a] m is the slope of the urea-induced transition region in cal/(mol·M). [b] $U_{50\%}$ is the urea concentration in M at the midpoint of urea denaturation. [c] T_m is the temperature at the midpoint of thermal denaturation in C. [d] ΔT is the width of the thermal phase transition in C.

circles. [Data for urea denaturation of $(R16)_{+8-4}$ (i.e., formerly "α16") were taken from the paper by Pantazatos and MacDonald (*18*).] Superposition of the CD_{222nm} and tryptophan fluorescence curves and the shapes of the curves themselves suggest that urea-induced unfolding in each case is a two-state transition. The pair of fragments in the middle panel of Figure 3, $(R16)_{00}$ and $(R16R17)_{00}$, are optimally phased according to X-ray crystal structures of two repeat fragments (*12*). Their common N-terminus begins the repeating heptad pattern in the first of the three helices of a repeat, whereas their C-termini are the last residues in the linker region immediately preceding the N-terminus of the next repeating unit in the cDNA sequence. The interrepeat linker region of five residues is clearly distinguishable in the X-ray crystal structures, as it does not conform to the repeating heptad pattern and serves to rotate the subsequent repeat around its long axis by 28° to 52° from the long axis of the previous repeat. Because the two repeats are not collinear, there is less steric hindrance to bending of the fragment at the linker region (*12*). In contrast with $(R16)_{00}$ and $(R16R17)_{00}$, the sequences of the pair in the top panel of Figure 3, $(R16)_{+8-4}$ and $(R16R17)_{+8-4}$, begin in repeat 15 and end four residues short of the crystallographically determined C-terminus (*12*). A third variation in phasing is given by the sequences of the pair in the bottom panel of Figure 3, $(R16)_{0+3}$ and $(R16R17)_{0+3}$, which begins with the crystallographically determined N-terminus of repeat 16 but ends three residues beyond the crystallographically determined C-terminus (*12*). Irrespective of the differences in their phasing, however, the single unit member of each of the three pairs of fragments unfolds at a lower urea concentration than the two-unit member of the same pair. To enable quantitative comparison of these curves, free energies of urea-induced unfolding (Table 2) were obtained by nonlinear regression fitting of the data in Figure 3 to eq 1 in Experimental Procedures, as indicated by the solid lines.

Thermodynamic Parameters of Urea-Induced Denaturation. Free energies of urea-induced denaturation, ΔG_{UN}s, obtained by fitting the data in Figure 3 by nonlinear regression to eq 1 (Experimental Procedures) are given in Table 2 to facilitate comparison with free energies of thermal denaturation to be considered subsequently. Related parameters of urea-induced denaturation—m, the slope of the transition, and $U_{50\%}$, the urea concentration at the midpoint of denaturation—are given in Table 3; both parameters, particularly m, are closely correlated with their associated free energies of unfolding. Urea-denatured peptides could be renatured (not shown), indicating that urea-induced unfolding is reversible as assumed in eq 1. As expected from superposition of the curves in Figure 3, free energies of urea denaturation, ΔG_{UN}s, derived from tryptophan fluorescence measurements and from CD_{222nm} measurements agreed within experimental error for all peptides. Based on these ΔG_{UN} values for urea denaturation monitored by CD_{222nm} and by tryptophan fluorescence in Table 2, thermodynamic stabilities increase in the order $(R16)_{00} = (R16)_{0+3} < (R16)_{+8-4} < (R16R17)_{+8-4} < (R16R17)_{00} < (R16R17)_{0+3}$. Thus, the single repeat of each pair is associated with a lower free energy of urea-induced unfolding than its two-repeat counterpart, although the magnitude of this difference varies from pair to pair. Despite differences in phasing which affect the stability of a peptide, therefore, a single repeat is less thermodynamically stable than its two-repeat counterpart.

Thermal Denaturation of Spectrin Peptides Monitored by Circular Dichroism at 222 nm. Although urea denaturation curves of one- and two-repeat fragments of spectrin were not superimposable (*17*) (Figure 3), heat denaturation curves of a cloned, single repeat and of intact spectrin dimers appeared to be superimposable (*19*). In a later study (*20*), the denaturation temperature of a fragment could not be correlated with the number of repeats in the fragment. To examine the apparent discrepancy between urea-induced and thermal unfolding in terms of free energies of unfolding of the peptides in Figure 3, each peptide unfolded with urea was also unfolded by heating from 5 or 10 °C to 85 °C. The CD_{222nm} of peptides at 1−3 μM in 10 mM sodium phosphate, pH 8, was monitored as the temperature was raised from 5 or 10 °C to 85 °C at a rate of 1° per min. After 85 °C had been attained, the samples were cooled to 10 or 25 °C, at which temperature the CD_{222nm} was measured to assess the extent of refolding. Since the net CD_{222nm} values of all cooled peptides were within 5−15% of that lost during temperature denaturation, the peptides were judged to have refolded on cooling. The fraction of unfolded values based on CD_{222nm} is plotted against the temperature in Figure 4. The shapes of the curves indicate that thermal unfolding is a two-state process. The top panel of Figure 4 shows that the thermal denaturation curves of $(R16)_{+8-4}$ and $(R16R17)_{+8-4}$ seem to be superimposable, but close inspection indicates that the former has a lower slope than the latter. The middle and bottom panels of Figure 4 show that thermal denaturation curves of the pairs, $(R16)_{00}$ and $(R16R17)_{00}$ and $(R16)_{0+3}$ and $(R16R17)_{0+3}$, respectively, are clearly not superimposable. The solid curves in Figure 4 represent the nonlinear regression fit of the data to eq 4 in Experimental Procedures.

Thermodynamic Parameters of Thermal Denaturation. Since thermal denaturation appears to be a reversible, two-state process for each fragment, the free energy of heat-induced unfolding of each fragment could be obtained by fitting the data in Figure 4 to eq 4 to extract the parameters, T_m and ΔT (Table 3), which were then used to solve for ΔG_{UN} in eq 5 (Experimental Procedures). The ΔG_{UN} of thermal unfolding of each peptide in Table 2 is within or near its corresponding $\Delta G_{UN} \pm$ standard error of urea denaturation in Table 2. Although this agreement indicates that heat capacity effects on ΔG_{UN} of these peptides are minimal, in contrast to what might be expected (*27*, *28*), we

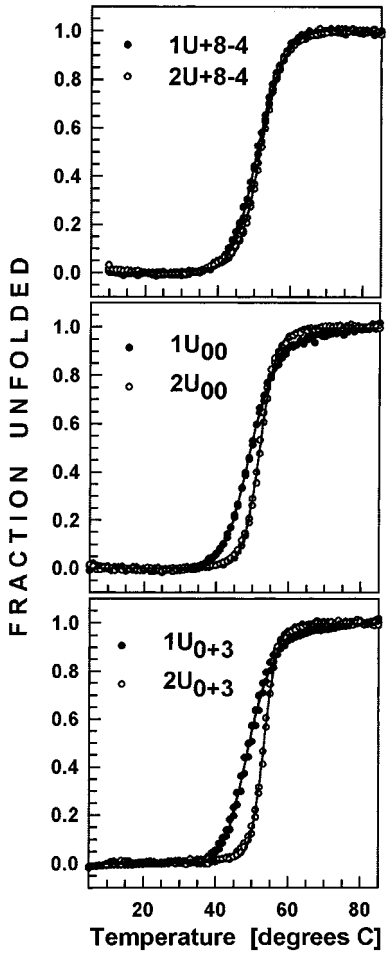

FIGURE 4: Fraction unfolded values calculated from CD_{222nm} of $(R16)_{+8-4}$, $(R16R17)_{+8-4}$, $(R16)_{00}$, $(R16R17)_{00}$, $(R16)_{0+3}$, and $(R16R17)_{0+3}$ plotted against temperature with a curve (solid line) describing the best fit of the data to eq 4 (Experimental Procedures). Closed circles represent two-repeat fragments, and open circles represent one-repeat fragments.

estimated the change in heat capacity of unfolding, ΔC_p^{UNF}, of each protein in two ways. First, we obtained the second derivative of the transition region to calculate $\Delta\Delta G_{UN}$, the maximum change in free energy attributable to the heat capacity. ΔC_p^{UNF} derived in this way had no significant effects on the free energies listed in Table 2. Second, as suggested by one of the reviewers and based on a previously described method (*27*, *28*), heat denaturation of each protein was performed in the presence of urea at a concentration just below that necessary to induce unfolding at room temperature. Enthalpies of the transition were obtained from a van't Hoff plot of these data and of the original heat denaturation data obtained in the absence of urea. The slope of the two enthalpies plotted against the associated transition temperatures for each protein gave the following ΔC_p^{UNF} estimates and corresponding percent decreases in ΔG_{UN} in parentheses due to these ΔC_p^{UNF} and T_ms in the absence of urea: 1.4 kcal mol^{-1} deg^{-1} (16%) for $(R16)_{+8-4}$, 0.2 kcal mol^{-1} deg^{-1} (4%) for $(R16R17)_{+8-4}$, 1.1 kcal mol^{-1} deg^{-1} (17%) for $(R16)_{00}$, 0.37 kcal mol^{-1} deg^{-1} (5%) for $(R16R17)_{00}$, 1.1 kcal mol^{-1} deg^{-1} (8%) for $(R16)_{0+3}$, 0.67 kcal mol^{-1} deg^{-1} (6%) for $(R16R17)_{0+3}$, 1.05 kcal mol^{-1} deg^{-1} (24%) for $(R16)_{+8+3}$, and 1.67 kcal mol^{-1} deg^{-1} (21%) for $(R16R17)_{0+9}$. Hence, omission of ΔC_p^{UNF} from the calculation of ΔG_{UN}s of thermal unfolding did not materially affect the order of the latter values, according to both methods used to estimate ΔC_p^{UNF}.

The T_ms of all peptides ranged from 49 to 54 °C (Table 3) and are close to the 49 °C first reported as the temperature of spectrin unfolding in intact red cells and red cell ghosts (*29*) and later observed to be the temperature of unfolding of intact spectrin dimers isolated from red cells (*30*). As found for ΔG_{UN} values for urea denaturation monitored by CD_{222nm} and by tryptophan fluorescence (Table 2), conformational stabilities indicated by ΔG_{UN} values for thermal denaturation (Table 2) increase in the order $(R16)_{00} = (R16)_{0+3} < (R16)_{+8-4} < (R16R17)_{+8-4} < (R16R17)_{00} < (R16R17)_{0+3}$. This trend is seen among T_m values and particularly among ΔT values (Table 3). Hence, by temperature-induced unfolding, as well as by urea-induced unfolding, single repeats of spectrin are thermodynamically less stable than identically phased, two-repeat fragments of spectrin. It is emphasized that this conclusion is supported even in the case of the pair, $(R16)_{+8-4}$ and $(R16R17)_{+8-4}$, with close to superimposable thermal denaturation curves in the top panel of Figure 4 but clearly different ΔG_{UN}s of unfolding in Table 2.

Effect on Stability of Peptide Extension at the C-Terminus. In addition to the greater stability of a fragment composed of two instead of one repeat, denaturation curves in Figures 3 and 4 and ΔG_{UN} values in Table 2 indicated that the phasing of $(R16R17)_{+8-4}$ gave a less thermodynamically stable peptide than $(R16R17)_{00}$ and $(R16R17)_{0+3}$. However, comparison of the corresponding single unit fragments, $(R16)_{+8-4}$, $(R16)_{00}$, and $(R16)_{0+3}$, indicated the opposite trend—i.e., $(R16)_{00}$ and $(R16)_{0+3}$, the N- and C-termini of which are optimally phased according to the X-ray crystal structures of two repeats (*12*), exhibited a slightly lower thermodynamic stability than $(R16)_{+8-4}$. To test whether the addition at the C-terminus of $(R16)_{0+3}$ is destabilizing, a seven-residue extension was added to $(R16)_{+8-4}$, creating $(R16)_{+8+3}$. As seen in the lower two panels of Figure 5, the unfolding of this seventh construct, $(R16)_{+8+3}$—whether induced by urea (Figure 5C) or by heating (Figure 5D)—appeared to be a two-state process as in the case of the first three pairs of peptides (Figures 3 and 4). Furthermore, its free energies of unfolding induced by urea and by heating revealed $(R16)_{+8+3}$ to be the thermodynamically most stable one-repeat fragment and almost as stable as $(R16R17)_{+8-4}$. Given the apparently stabilizing effect of the extension of the C-terminus of $(R16)_{+8-4}$, we also tested the effect of C-terminus extension of the most stably folded two-unit fragment, $(R16R17)_{0+3}$, by creating $(R16R17)_{0+9}$. As seen in the upper two panels of Figure 5, the unfolding of this eighth construct, $(R16R17)_{0+9}$, whether induced by urea (Figure 5A) or by heating (Figure 5B), also appeared to be a two-state process. In the case of $(R16R17)_{0+3}$, however, C-terminus extension decreased, instead of increasing, the stability of $(R16R17)_{0+9}$, which, with a free energy of 7.9 kcal/mol, was thermodynamically less stable than $(R16R17)_{0+3}$ with a free energy of 9.9 kcal/mol.

Derivation of the Free Energy of Denaturation of a Two-Repeat Peptide Occurring by Independent Unfolding of Each Repeat. At the outset of this investigation it was unclear whether denaturation of a two-repeat peptide occurs by coupled denaturation of both repeats or by the denaturation

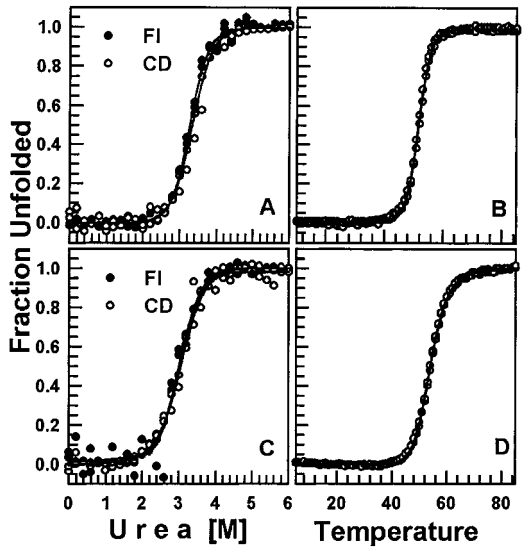

FIGURE 5: (A) Fraction unfolded values of $(R16R17)_{0+9}$ plotted against urea concentration with a curve (solid line) describing the best fit of the data to eq 1 (Experimental Procedures). Open circles represent CD_{222nm} data, and closed circles represent tryptophan fluorescence data. (B) Fraction unfolded values based on CD_{222nm} of $(R16R17)_{0+9}$ plotted against temperature with a curve (solid line) describing the best fit of the data to eq 4 (Experimental Procedures). (C) Fraction unfolded values of $(R16)_{+8+3}$ plotted against urea concentration with a curve (solid line) describing the best fit of the data to eq 1 (Experimental Procedures). Open circles represent CD_{222nm} data, and closed circles represent tryptophan fluorescence data. (D) Fraction unfolded values based on CD_{222nm} of $(R16)_{+8+3}$ plotted against temperature with a curve (solid line) describing the best fit of the data to eq 4 (Experimental Procedures).

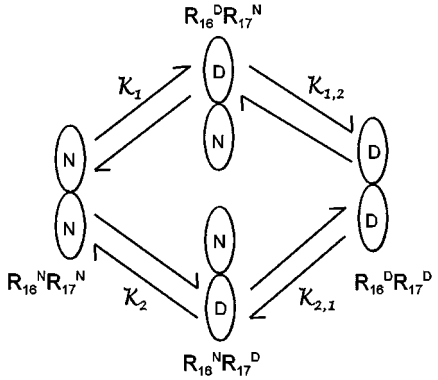

FIGURE 6: Diagram of the pathway of independent denaturation of each unit of a fragment of repeats 16 and 17 of chicken brain α-spectrin illustrating the derivation in the Appendix in which it is assumed that $k_1 = k_2 = k_{1,2} = k_{2,1}$. The diagram includes intermediates of unfolding consisting of half-denatured forms in which each ellipse represents a single repeat, either native (N) or denatured (D). This pathway is not supported by the results in this paper.

of each repeat independently. It seemed intuitively reasonable that in the latter case the free energy of denaturation of a two-repeat fragment would be the same as the free energy of denaturation of a single repeat, the opposite of which was observed. To determine whether the free energy of denaturation of a two-repeat fragment, in which each repeat denatures independently, should indeed be the same as that of an isolated, single repeat, we undertook the derivation of this parameter, which is given in the Appendix. According to this scenario, the diagram in Figure 6 depicts a two-repeat peptide as it undergoes complete unfolding through two intermediate states, in which different halves of the peptide are denatured. As seen in the last step of the derivation in the Appendix, the equilibrium constant, $K_{exptl\theta,}$ for the denaturation process in Figure 6, is equal to $[k(1 + k)/(1 + k)]$ and reduces to k, which is equal to k_1, k_2, k_{12}, and k_{21}, the rate constants of each progressive and independent denaturation of a repeat leading to complete denaturation of a two-repeat fragment. Hence, the free energy of denaturation of a two-repeat fragment occurring by independent unfolding of each repeat, $\Delta G^{\circ}_{\text{two repeat}}$, is $= -RT \ln k$ and, therefore, the same as that of a single repeat, which is contrary to our finding of a greater free energy of unfolding of a two-repeat fragment compared with a single repeat. Therefore, two repeats fold in concert and not independently.

DISCUSSION

Two-Repeat Fragments Are Thermodynamically More Stable Than a Single Repeat. Cloned fragments of two tandem repeats of spectrin are thermodynamically more stable than identically phased, cloned fragments of a single repeat, according to the greater free energies of both urea denaturation and thermal denaturation of the former than the latter (Table 2). Thus, the apparent discrepancy between *nonoverlapping* urea denaturation curves of one and multiple repeat fragments of spectrin (*17*), on one hand, versus *overlapping* thermal denaturation curves of a single repeat and intact spectrin dimers (*19*), on the other hand, can be resolved by comparing the ΔG_{UN}s of urea denaturation and the ΔG_{UN}s of thermal denaturation. These ΔG_{UN}s are the same within experimental error for each peptide (Table 2) and indicate clearly that two-repeat fragments are thermodynamically more stable than a single repeat. An example of deceptively similar thermal denaturation curves was also encountered in this investigation on comparison of heat denaturation curves of the single repeat $(R16)_{+8-4}$ and the identically phased two-repeat peptide $(R16R17)_{+8-4}$ (top panel of Figure 4). Close examination shows, however, that the slope of the single repeat is lower than that of the two-repeat peptide, as borne out by the lower free energy of thermal denaturation of the single-repeat than the two-repeat peptide (Table 2). As in all cases, parameters reflecting the degree of cooperative behavior (Table 3)—i.e., m, the slope of the transition region, in a urea denaturation curve and ΔT, the width of the transition region, in a thermal denaturation curve—seem to be more consistent correlates of their related free energy values than $U_{50\%}$, the urea concentration at the midpoint of urea denaturation, and T_m, the temperature at the midpoint of thermal denaturation. The data presented here attest to the reliability of both chemical and thermal denaturation as a means of assessing the thermodynamic stabilities of these particular peptides, as have earlier investigations of other proteins—for example, *Staphylococcus aureus* nuclease A (*31*), thioredoxin (*32*), RNase A (*33*), and chymotrypsin inhibitor 2 (*24*).

Reasons for the Free Energy Differences between Identically Phased One- and Two-Repeat Members of Each Pair of Spectrin Fragments. The greater thermodynamic stability of two repeats than a single repeat appears to reflect differences in tertiary, as opposed to secondary, structure, since there was no correlation between the mean residue ellipticity of a peptide, on one hand, and its number of repeats (Table 1) or free energies of unfolding (Table 2), on the other

hand. Free energy differences between one- and two-repeat members of pairs of identically phased spectrin fragments might be attributed to differences in the sequences of their C-terminal ends or to structural features possessed by the two-repeat fragment but not by the single repeat. To evaluate the likelihood of the former alternative, the C-terminal sequences were examined for helix-capping motifs which might prove sufficiently stabilizing or destabilizing, as indicated by normalized positional residue frequencies determined at C-terminal ends (*34*), to account for the observed differences in free energies of unfolding between identically phased one and two repeats. No such helix-capping motifs were found. Although residues of relatively low helix propensity (*35*, *36*) do occur in the C-termini of $(R16)_{+8-4}$, $(R16)_{00}$, and $(R16R17)_{00}$, their distribution could not account for the consistently more stable folding of two-repeat fragments than single repeats. Alternatively, a structural basis is more likely for these free energy differences with magnitudes of 1.6 kcal/mol for the pair, $(R16)_{+8-4}$ and $(R16R17)_{+8-4}$, 4.6 kcal/mol for the optimally phased pair, $(R16)_{00}$ and $(R16R17)_{00}$, and 6.2 kcal/mol for the pair, $(R16)_{0+3}$ and $(R16R17)_{0+3}$. For example, these free energies could signify the presence of one or more hydrogen bonds in the two-repeat fragment, which is absent from the identically phased single repeat and confers greater stability on the two-repeat fragment as found in a number of proteins (e.g., refs *37* and *38*). Evidence for such hydrogen bonds has been observed in the X-ray crystal structure of $(R16R17)_{0+3}$ (*12*) in the form of hydrogen bond distances from the side chain of serine 1874 in the linker region between R16 and R17 to the side chains of histidine 1947 and histidine 1948 in the BC loop between the second and third α-helices of R17. Since $(R16)_{0+3}$ includes a linker region but not the BC loop between the second and third α-helices of the following repeat, $(R16)_{0+3}$ is missing these hydrogen bonds and would be less stable than $(R16R17)_{0+3}$, assuming no other structural differences between the R16 regions of the two peptides. Structural differences between the R16 regions of $(R16)_{+8-4}$ and $(R16R17)_{+8-4}$ have been observed, however, in that the first nine N-terminal residues of $(R16)_{+8-4}$ adopt the conformation of a random coil by NMR (*9*, *10*) but some of the same N-terminal residues—i.e., the third to ninth—of $(R16R17)_{+8-4}$ form an α-helix by X-ray crystallography.

The larger *m* values for two-unit than for one-unit fragments (Table 3) parallel the larger amounts of helix in and greater surface-accessible areas of the two-unit than one-unit fragments, as expected. For example, the surface-accessible area obtained by X-ray crystallography (*12*) for $(R16R17)_{00}$ with an *m* value of 2506 cal/(mol·M) and an $M_{w,app}$ of 24 312 Da is 12 379 Å^2, nearly twice the 6440 Å^2 obtained by NMR (*9*, *10*) for $(R16)_{+8-4}$ with an *m* value of 1960 cal/(mol·M) and an $M_{w,app}$ of 12 803 Da. Thus, the surface-accessible areas of cloned spectrin repeats appear similar to those of globular proteins—e.g., 6710 Å^2 for lysozyme and 7010 Å^2 for ribonuclease S with $M_{w,app}$s of 14 300 and 13 700 Da, respectively (*39*). More insight into the structures and observed, greater thermodynamic stabilities of two-repeat fragments than single repeats may be provided in the future by ΔC_p^{UNF} values determined by calorimetry. Although sufficiently accurate to indicate their relatively negligible effects on ΔG_{UN}, the estimated ΔC_p^{UNF}s given in the Results are puzzling in that larger ΔC_p^{UNF}s were given by single units than by two-unit fragments, contrary to expectation from values for *m* and the surface-accessible area.

Reasons for Differences in Phasing Having Different Effects among Single Repeats Than among Two-Repeat Fragments. The lower stabilities of $(R16)_{00}$ and of $(R16)_{0+3}$ than $(R16)_{+8-4}$ were surprising, since the identically phased two-repeat constructs without eight additional residues at the N-terminus and with four fewer residues at the C-terminus, $(R16R17)_{00}$ and $(R16R17)_{0+3}$, were more thermodynamically stable than $(R16R17)_{+8-4}$ (Table 2). The latter result was expected since—as indicated above—the first nine N-terminal residues of $(R16)_{+8-4}$ adopted a random coil, as opposed to α-helical, conformation in the NMR structure of this single repeat (*9*, *10*) and the first two N-terminal residues of $(R16R17)_{+8-4}$ also adopted a random coil conformation in the X-ray crystal structure of this fragment, whereas the N-terminal regions of two-repeat constructs beginning in the "0" position are entirely α-helical (*12*). Again, these opposite effects of the same phasing differences among single repeats compared with two-repeat fragments do not appear to be accounted for by the presence of stabilizing or destabilizing helix-capping motifs (*34*) or residues with unusual helix propensities at the N- or C-termini (*35*, *36*). Pertaining to the single repeats alone, one explanation for the greater stability of $(R16)_{+8-4}$ than of $(R16)_{00}$ and $(R16)_{0+3}$ is the inclusion in the former of the linker region of R15 at the N-terminal end, which could form hydrogen bonds with the BC loop between the second and third α-helices of R16 and thereby cause $(R16)_{+8-4}$ to be more stably folded than $(R16)_{00}$ and $(R16)_{0+3}$. An alternative possibility that the seven-residue C-terminal extension on $(R16)_{0+3}$ is destabilizing is ruled out by the greater stability of $(R16)_{+8+3}$ with a ΔG_{UN} of 5.9 kcal/mol than $(R16)_{+8-4}$ with a ΔG_{UN} of 4.4 kcal/mol (Figure 4, Table 3). However, if hydrogen bonds do exist between the eight extra N-terminal residues and the BC loop of $(R16)_{+8-4}$, as in $(R16R17)_{0+3}$, and do account for the greater stability of $(R16)_{+8-4}$ than $(R16)_{00}$ and $(R16)_{0+3}$, it becomes unclear why $(R16R17)_{+8-4}$ is less thermodynamically stable than $(R16R17)_{00}$ and $(R16R17)_{0+3}$, since each then would possess stabilizing hydrogen bonds. Another obviously stabilizing feature in the X-ray crystal structures of $(R16R17)_{00}$ and $(R16R17)_{0+3}$ is the coterminal arrangement of the ends of the three α-helices of R17, whereas those of $(R16R17)_{+8-4}$ are not coterminal (*12*). Understanding of the observed differences in thermodynamic stabilities will require more detailed structural information.

Evidence for "Fraying". The greater thermodynamic stability of $(R16R17)_{0+3}$ than $(R16R17)_{00}$ may be due to the presence in the former of additional terminal residues which prevent "fraying" of the α-helix at the C-terminus (*40*). Likewise, an increase in the free energies of denaturation of peptides cloned from spectrin-related dystrophin was obtained by increasing the length of the construct to 123 residues (*41*, *42*), well beyond the 109 residues identified as the length of a dystrophin repeat from DNA sequence analysis (*43*). The notion of fraying is in agreement with the destabilizing effect of further extension of $(R16R17)_{0+3}$ by nine residues at the C-terminus, resulting in $(R16R17)_{0+9}$ with a lower ΔG_{UN} than that of $(R16R17)_{0+3}$. In other words, extension of the C-terminus beyond that necessary to prevent

fraying does not result in increased thermodynamic stability. As observed in the crystal structure of $(R16R17)_{0+9}$ (*12*), the helical, nine-residue extension protrudes from the C-terminal end of $(R16R17)_{0+9}$, unable to engage in stabilizing interactions with other helices as it would within a complete repeat. The helical conformation of and presence of a tryptophan on the nine-residue extension of $(R16R17)_{0+9}$ are supported by $(R16R17)_{0+9}$ exhibiting the same mean residue ellipticity at 222 nm as all other fragments (Table 1) but an unshielded, as well as a shielded, tryptophan (Figure 2B). Again, there were no stabilizing or destabilizing helix-capping motifs at the C-terminus of $(R16R17)_{0+9}$ (*34*) or residues with unusual helix propensities at the N- or C-termini (*35*, *36*), which might account for its reduced thermodynamic stability.

Comparison between Mechanical Unfolding of Spectrin Repeats and Unfolding of Spectrin Repeats by Thermal and Urea Denaturation. Since the denatured state induced by mechanical unfolding—i.e., an extended chain—should differ from that induced by chemical denaturants and temperature—i.e., a random coil conformation in solution—unfolding caused by these two agents might be expected to proceed by different pathways, as suggested by results of molecular dynamics simulation (*44*). Although strict extrapolation from the latter to experiment has its uncertainties, differences between the mechanical unfolding of spectrin and α-actinin fragments investigated with the atomic force microscope (*45*, *46*) and unfolding induced by heating (*19*, *20*, and as reported here) and by urea (*17* and as reported here) appear to bear out the predictions of molecular dynamics simulation. Initially, force-extension patterns obtained by atomic force microscopy indicated that single repeats of spectrin and α-actinin unfold independently (*45*). In a recent, more detailed study (*46*) a bimodal distribution of lengths of unfolding has been interpreted as evidence for the existence of intermediate, as well as fully folded and fully unfolded, states of fragments of multiple repeats of spectrin with identical or with different sequences. On heating or exposure to urea, in contrast, the repeats in a two-repeat spectrin fragment appear to unfold in concert and not independently, since they have greater free energies of unfolding than identically phased single repeats. It is recalled that independently folding repeats should have the same free energies of unfolding, according to the derivation in the Appendix. A final difference between mechanical unfolding, on the one hand, and heat- and urea-induced unfolding, on the other hand, is the lack of evidence thus far for intermediate states in the latter processes.

Relevance of Free Energy Measurements for the Understanding of Spectrin Flexibility. Destabilized states of proteins are of interest not only in the context of the energetics of protein folding but also for their potential contribution to the understanding of the function of those proteins (*47*). Both considerations justify the study of perturbations of the native structure of spectrin which are fundamental to the flexibility that is its hallmark. Spectrin flexibility has been suggested on the basis of conformational changes inferred from X-ray crystal structures of two-repeat fragments of chicken brain α-spectrin to involve bending of the repeating unit domain of spectrin at linker regions and/or conformational rearrangements of loop and helix regions of spectrin repeats (*12*). In the present investigation, a type of cooperative unfolding has been unequivocally demonstrated which involves inter-repeat interactions. It is tempting to infer the relevance of such interactions to network-destabilizing effects of spectrin mutations which are clinically correlated with hemolytic anemia but located far from the spectrin self-association site (*48*). More dramatic changes, such as reversible unfolding of single, coiled-coil repeats of spectrin and α-actinin observed by atomic force microscopy (*45*, *46*) and inferred extension of spectrin by micropipet aspiration (*49*), suggest other paradigms of spectrin flexibility (*50*). In addition to results obtained with the above experimental approaches, the results reported here of significant effects of modest differences in phasing on the free energies of unfolding of spectrin fragments add to the by now amply documented (*12*, *17*, *19*, *20*, *51*, *52*) possibilities for refinement of the original concept of "phasing" (*14*) of spectrin repeats, giving further scope to future investigations of the structure and function of spectrin and related cytoskeletal proteins.

ACKNOWLEDGMENT

We thank Weina Niu, Woo Kim, and Julie Ruffatti for excellent technical assistance, Ann Kochuveli and Flora Lwin for laboratory assistance, Matti Saraste for the generous gift of the cDNA of chicken brain α-spectrin, Katharina Spiegel, Andrew Murphy, and Joshua Hays of the Keck Facility of the Department of Biochemistry, Molecular Biology and Cell Biology of Northwestern University for excellent instrument support, Richard Milberg of the University of Illinois at Urbana-Champaign and Fenghe Qiu of Northwestern University for mass spectrometry analysis, Janelle Thorek of the Biotechnology Facility at Northwestern University for assistance with cDNA sequencing, Francis Neuhaus for use of his sonicator and incubator, Irving Klotz for help with the derivation of the free energy of independent denaturation of single repeats in a two-repeat fragment, and Robert MacDonald, Alfonso Mondragón, Brian Shoichet, and Jonathan Widom for suggestions and for reading the manuscript.

APPENDIX

Denaturation of a two-repeat peptide is assumed to begin in either of the two repeats, as shown in Figure 6, so that $R16_NR17_N$ undergoes a transition to either $R16_DR17_N$ or $R16_NR17_D$, each of which is characterized by the equilibrium constant, k_1 or k_2, respectively. Each partially denatured peptide, $R16_DR17_N$ or $R16_NR17_D$, will undergo a further transition to the completely denatured form, $R16_DR17_D$, each of which is characterized by the equilibrium constant, $k_{1,2}$ or $k_{2,1}$, respectively. Thus, the equilibrium constant, K_1, for the first half of the denaturation process is described by the equation

$$K_1 = [(R16_DR17_N) + (R16_NR17_D)]/(R16_NR17_N) = k_1 + k_2 \quad (6)$$

and the equilibrium constant, K_2, for the second half of the denaturation process is described by the equation

$$K_2 = (R16_DR17_D)/[(R16_DR17_N) + (R16_NR17_D)] \quad (7)$$

K_2 is inverted in order to equate it with its equilibrium constants, $k_{1,2}$ and $k_{2,1}$:

$$1/K_2 = [(R16_DR17_N) + (R16_NR17_D)]/(R16_DR17_D) = 1/k_{1,2} + 1/k_{2,1} = (k_{2,1} + k_{1,2})/k_{1,2}k_{2,1} \quad (8)$$

Therefore

$$K_2 = k_{1,2}k_{2,1}/(k_{2,1} + k_{1,2}) \quad (9)$$

If one reasonably assumes that $k_1 = k_2 = k_{1,2} = k_{2,1} \equiv k$, i.e., that each repeat in a two-repeat peptide is independent of the other and unfolds with the same k when it is a single-repeat peptide, then

$$K_1K_2 = k^2 = (R16_DR17_D)/(R16_NR17_N) \quad (10)$$

To derive an equilibrium constant, $K_{exptl\theta}$, in terms of a signal, θ, which changes on denaturation, a two-state model is assumed which is represented as

$$K_{exptl\theta} = \alpha/(1 - \alpha) \quad (11)$$

Since $R16_DR17_N$ and $R16_NR17_D$ are half-denatured, they must contribute to θ, but half as much as an equimolar concentration of $R16_DR17_D$, given that θ increases with denaturation. Thus

$$K_{exptl\theta} = [{}^1/_2(R_{16}{}^DR_{17}{}^N) + {}^1/_2(R_{16}{}^NR_{17}{}^D) + (R_{16}{}^DR_{17}{}^D)]/[(R_{16}{}^NR_{17}{}^N) + {}^1/_2(R_{16}{}^DR_{17}{}^N) + {}^1/_2(R_{16}{}^NR_{17}{}^D)] \quad (12)$$

Substituting to express the equation in terms of $R_{16}{}^NR_{17}{}^N$

$$K_{exptl\theta} = [{}^1/_2(k_1R_{16}{}^NR_{17}{}^N) + {}^1/_2(k_2R_{16}{}^NR_{17}{}^N) + (k_1k_{12}R_{16}{}^NR_{17}{}^N)]/[(R_{16}{}^NR_{17}{}^N) + {}^1/_2(k_1R_{16}{}^NR_{17}{}^N) + {}^1/_2(k_2R_{16}{}^NR_{17}{}^N)] \quad (13)$$

Eliminating $R_{16}{}^NR_{17}{}^N$ and consolidating, since $k_1 = k_2 = k_{12} = k_{21}$

$$K_{exptl\theta} = [k(1 + k)/(1 + k)] = k \quad (14)$$

$$\Delta G^\circ{}_{\text{two repeat}} = -RT \ln k \quad (15)$$

Therefore, the free energy of unfolding of a two-repeat peptide occurring by independent unfolding of each repeat should be the same as the free energy of unfolding of a single repeat.

REFERENCES

1. Bennett, V., and Gilligan, D. M. (1993) *Annu. Rev. Cell Biol. 9*, 27−66.
2. Winkelmann, J. C., and Forget, B. G. (1993) *Blood 81*, 3173−3185.
3. Lux, S. E., and Palek, J. (1995) in *Blood: Principles and Practice of Hematology* (Handin, R. I., Lux, S. E., and Stossel, T. B., Eds.) pp 1701−1818, J. B. Lippincott Co., Philadelphia, PA.
4. Beck, K. A., and Nelson, W. J. (1996) *Am. J. Physiol 270*, C1263−C1270.
5. De Matteis, M. A., and Morrow, J. S. (2000) *J. Cell Sci. 113* (Part 13), 2331−2343.
6. Dubreuil, R. R. (1996) in *Current Topics in Membranes* (Nelson, W. J., Ed.) pp 147−167, Academic Press, San Diego.
7. Speicher, D. W., and Marchesi, V. T. (1984) *Nature 311*, 177−180.
8. Yan, Y., Winograd, E., Viel, A., Cronin, T., Harrison, S. C., and Branton, D. (1993) *Science 262*, 2027−2030.
9. Pascual, J., Pfuhl, M., Rivas, G., Pastore, A., and Saraste, M. (1996) *FEBS Lett. 383*, 201−207.
10. Pascual, J., Pfuhl, M., Walther, D., Saraste, M., and Nilges, M. (1997) *J. Mol. Biol. 273*, 740−751.
11. Parry, D. A., Dixon, T. W., and Cohen, C. (1992) *Biophys. J. 61*, 858−867.
12. Grum, V. L., Li, D., MacDonald, R. I., and Mondragon, A. (1999) *Cell 98*, 523−535.
13. Djinovic-Carugo, K., Young, P., Gautel, M., and Saraste, M. (1999) *Cell 98*, 537−546.
14. Winograd, E., Hume, D., and Branton, D. (1991) *Proc. Natl. Acad. Sci. U.S.A. 88*, 10788−10791.
15. Viel, A., and Branton, D. (1996) *Curr. Opin. Cell Biol. 8*, 49−55.
16. Pascual, J., Castresana, J., and Saraste, M. (1997) *BioEssays 19*, 811−817.
17. Menhart, N., Mitchell, T., Lusitani, D., Topouzian, N., and Fung, L. W. (1996) *J. Biol. Chem. 271*, 30410−30416.
18. Pantazatos, D. P., and MacDonald, R. I. (1997) *J. Biol. Chem. 272*, 21052−21059.
19. DeSilva, T. M., Harper, S. L., Kotula, L., Hensley, P., Curtis, P. J., Otvos, L., Jr., and Speicher, D. W. (1997) *Biochemistry 36*, 3991−3997.
20. Lusitani, D., Menhart, N., Keiderling, T. A., and Fung, L. W. (1998) *Biochemistry 37*, 16546−16554.
21. Lecomte, M. C., Nicolas, G., Dhermy, D., Pinder, J. C., and Gratzer, W. B. (1999) *Eur. Biophys. J. 28*, 208−215.
22. Wasenius, V. M., Saraste, M., Salven, P., Eramaa, M., Holm, L., and Lehto, V. P. (1989) *J. Cell Biol. 108*, 79−93.
23. MacDonald, R. I., Musacchio, A., Holmgren, R. A., and Saraste, M. (1994) *Proc. Natl. Acad. Sci. U.S.A. 91*, 1299−1303.
24. Jackson, S. E., Moracci, M., elMasry, N., Johnson, C. M., and Fersht, A. R. (1993) *Biochemistry 32*, 11259−11269.
25. Cantor, C. R., and Schimmel, P. R. (1980) in *Biophysical Chemistry*, pp 1075−1107, W. H. Freeman and Co., New York.
26. Greenfield, N., and Fasman, G. D. (1969) *Biochemistry 8*, 4108−4116.
27. Becktel, W. J., and Schellman, J. A. (1987) *Biopolymers 26*, 1859−1877.
28. Pace, C. N., Shirley, B. A., and Thomson, J. A. (1989) in *Protein Structure: A Practical Approach* (Creighton, T., Ed.) pp 311−330, IRL Press at Oxford University Press, Oxford.
29. Brandts, J. F., Erickson, L., Lysko, K., Schwartz, A. T., and Taverna, R. D. (1977) *Biochemistry 16*, 3450−3454.
30. Yoshino, H., and Marchesi, V. T. (1984) *J. Biol. Chem. 259*, 4496−4500.
31. Eftink, M. R., Ghiron, C. A., Kautz, R. A., and Fox, R. O. (1991) *Biochemistry 30*, 1193−1199.
32. Santoro, M. M., and Bolen, D. W. (1992) *Biochemistry 31*, 4901−4907.
33. Yao, M., and Bolen, D. W. (1995) *Biochemistry 34*, 3771−3781.
34. Aurora, R., and Rose, G. D. (1998) *Protein Sci. 7*, 21−38.
35. Chakrabartty, A., and Baldwin, R. L. (1995) *Adv. Protein Chem. 46*, 141−176.
36. Pace, C. N., and Scholtz, J. M. (1998) *Biophys. J. 75*, 422−427.
37. Myers, J. K., and Pace, C. N. (1996) *Biophys. J. 71*, 2033−2039.
38. Peterson, R. W., Nicholson, E. M., Thapar, R., Klevit, R. E., and Scholtz, J. M. (1999) *J. Mol. Biol. 286*, 1609−1619.
39. Lee, B., and Richards, F. M. (1971) *J. Mol. Biol. 44*, 379−499.
40. Kohn, W. D., Kay, C. M., and Hodges, R. S. (1998) *J. Mol. Biol. 283*, 993−1012.

41. Kahana, E., and Gratzer, W. B. (1995) *Biochemistry 34*, 8110−8114.
42. Calvert, R., Kahana, E., and Gratzer, W. B. (1996) *Biophys. J. 71*, 1605−1610.
43. Koenig, M., Monaco, A. P., and Kunkel, L. M. (1988) *Cell 53*, 219−226.
44. Paci, E., and Karplus, M. (2000) *Proc. Natl. Acad. Sci. U.S.A. 97*, 6521−6526.
45. Rief, M., Pascual, J., Saraste, M., and Gaub, H. E. (1999) *J. Mol. Biol. 286*, 553−561.
46. Lenne, P. F., Raae, A. J., Altmann, S. M., Saraste, M., and Horber, J. K. (2000) *FEBS Lett. 476*, 124−128.
47. Dill, K. A., and Shortle, D. (1991) *Annu. Rev. Biochem. 60*, 795−825.
48. Marchesi, S. L., Letsinger, J. T., Speicher, D. W., Marchesi, V. T., Agre, P., Hyun, B., and Gulati, G. (1987) *J. Clin. Invest. 80*, 191−198.
49. Lee, J. C., Wong, D. T., and Discher, D. E. (1999) *Biophys. J. 77*, 853−864.
50. Discher, D. E. (2000) *Curr. Opin. Hematol. 7*, 117−122.
51. Lusitani, D. M., Qtaishat, N., LaBrake, C. C., Yu, R. N., Davis, J., Kelley, M. R., and Fung, L. W. (1994) *J. Biol. Chem. 269*, 25955−25958.
52. Nicolas, G., Pedroni, S., Fournier, C., Gautero, H., Craescu, C., Dhermy, D., and Lecomte, M. C. (1998) *Biochem. J. 332* (Part 1), 81−89.

BI0025159